8A.8 THE "OWL HORN" RADAR SIGNATURE IN DEVELOPING SOUTHERN-PLAINS THUNDERSTORMS

Matthew R. Kramar* and Howard B. Bluestein
Univ. of Oklahoma
Norman, Oklahoma

Andrew L. Pazmany
Univ. of Massachusetts
Amherst, Massachusetts

John D. Tuttle
NCAR
Boulder, Colorado

1. INTRODUCTION

Using a mobile, 3 cm-wavelength radar system built by a group at the University of Massachusetts at Amherst, we have been able to survey supercell thunderstorms with a much finer spatial (and temporal) resolution possible than using the WSR-88D radars, because WSR-88D radars are at fixed sites, while we, being mobile, can consistently view storms at ranges of 10 to 20 km. Consequently, we are able to see features of supercell thunderstorms that might otherwise go unresolved. In the course of the 2001 severe storm season in the Central Plains, we first observed a curious, recurring reflectivity signature on our radar display which we have called the "Owl Horn" signature (because the radar reflectivity signature resembles the ears of an owl). The feature was apparent from various viewing angles with respect to the storms exhibiting the signature, thus eliminating the possibility that the feature was an artifact of the radar. The U. Mass. radar operated with an antenna beamwidth of 1.25 degrees, transmitted 1 microsecond pulses, and had a range resolution of 150m.

We have undertaken a study of the "Owl Horn" signature using the Tracking Radar Echoes by Correlation technique (TREC). We have found nothing in the literature that discusses the "Owl Horn" signature. Although TREC has previously been applied to clear air and hurricane environments (Tuttle and Foote 1990; Tuttle and Gall 1999), also absent from the literature is an application of TREC to severe storm and supercell evolution. Rinehart (1979), however, has studied internal storm motions by applying TREC to severe storms. Through the application of TREC to our radar reflectivity data (Doppler wind data were not available in 2001) during May and June, 2001, we compute the horizontal wind field around and in the "Owl Horn" signature.

Recently, we have discovered instances of the "Owl Horn" in numerical model storm simulations. In this paper we summarize the characteristics of the signature, identify conditions under which it occurs and discuss the results of our simulations.

2. THE TREC TECHNIQUE

The TREC technique is a pattern-recognition procedure applied to radar reflectivity data using a cross-correlational analysis. Radar-echo data are stored in arrays, and on each iteration an array is compared to all other arrays of the same size for the subsequent time step to determine which array exhibits the highest correlation with the previous array. The final array with the highest correlation is considered to be the endpoint of a motion vector beginning at the original array. The array size is an arbitrary input parameter in the program, but it is limited in range, since if it is too large, resolution is sacrificed, and if it is too small a trustworthy correlation coefficient may not be found (Tuttle and Gall 1999).

As illuminated by Tuttle and Foote (1990), a strong advantage to TREC is that only one radar is required, and the technique produces a wind field wherever there are reflectivity data. However, Rinehart (1979) found in a comparison of wind-field estimates in a convective storm from TREC with a dual-Doppler analysis of the wind field that there were significant differences, possibly owing to strong vertical motion, vertical shear, and rapid convective precipitation development as characterize thunderstorms, where advection no longer dominates.

Typically, the radar-echo data used in TREC are taken several minutes apart since ground-based WSR-88D radar data are obtained on roughly five minute scales. Since the mobile Doppler radar obtains data roughly every 20 seconds and our features of interest are on a much smaller time-scale than those of previous studies, we take advantage of our finer temporal spacing to refine the analysis in our study.

One hurdle to overcome in the TREC analysis was obtaining a storm-relative wind field. Since storm-motion data were lacking in our cases, we resolved the issue by a two-step TREC procedure. First we applied the TREC algorithm to the reflectivity data to obtain a ground-relative wind field. We then calculated the average u and v components of the wind field by averaging the u and v components of all of the individual calculated wind vectors and treated this averaged vector as the mean storm-motion vector. Finally, we re-ran the TREC algorithm and used as an input parameter our computed average mean storm motion vector, subtracting the motion vector out from each of the re-computed wind vectors before producing the output display.

3. RESULTS AND DISCUSSION

The "Owl Horn" signature is characterized by two protrusions from the rear side (with respect to storm motion) of the storm reflectivity, which seems first to appear when an isolated, somewhat organized storm intensifies. Temporally, the feature lasts no more than several minutes and disappears as the storm intesnifies. During the 2001 severe storm season in the Central Plains, we observed a well-defined "Owl Horn" signature on May 27 (west of Liberal, Kansas), May 28 (North of Raton Pass, New Mexico), May 29 (Turkey, Texas), and June 5 (near Woodward, Oklahoma). Indeed, the storms that exhibited the signature on May 28, May 29 and June 5 all developed

*Corresponding author address: Matthew R. Kramar, School of Meteorology, Univ. of Oklahoma, Norman, OK, 73019; email: mkramar@weather.ou.edu.

into supercells that produced funnel clouds or tornadoes. We can not know the future of the May 27 storm if it had remained isolated, as it was overtaken by a very strong outflow boundary from an MCS to its north before it could develop further.

In TREC analyses of both the May 27 and June 5 cases (Figures 1 and 2), there is a temporally consistent boundary of convergent winds which lasts from five to ten minutes and seems to partition the storm. A temporally-consistent downdraft based on a divergence signature is also apparent on the full storm analysis for each case, and leads us to suspect that the line of convergent winds represents an outflow boundary.

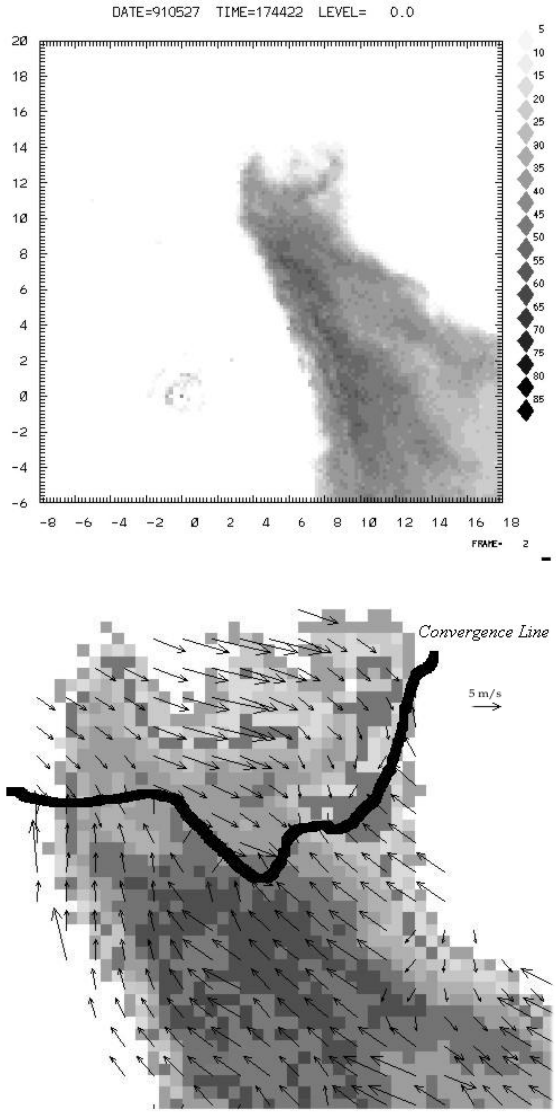

Figure 1: TREC storm-relative wind analysis from the May 27, 2001 case, 4:44pm CDT. The reflectivity signature (top) and an enlarged view of the "Owl Horn" region with the convergence line drawn. Distance in km, wind speed in ms^{-1}, reflectivity in dBZ, gridpoint spacing is 500m.

Using the Advanced Regional Prediction System (Xue, et al. 2000) model and the Del City composite sounding of May 20, 1977 along with a suite of constructed environmental profiles (Adlerman and Droegemeier 2002), we have made a numerical study of the "Owl Horn" in computer simulations. In the cases that produced an "Owl Horn" signature (Table 1; weaker- and stronger-shear cases did not produce "Owl Horn" signatures), we examine plots of several meteorological quantities.

Vertical cross-section plots of reflectivity show the formation of two separate precipitation shafts minutes prior to the onset of the "Owl Horn" reflectivity signature (Figure 3). This is in agreement with observations of storms exhibiting the signature. In plots of perturbation potential temperature (Figure 4a) it is seen that prior to the formation of the signature in reflectivity, two distinct cold pools develop, one on each side of the heaviest core of reflectivity, and that the "Owl Horns" are coincident with narrow protrusions of the coldest air contained in the outflow, thus verifying that the convergence line from TREC is likely an outflow boundary. Of interest, however, is a notch of relatively warmer air in between the pair of cold protrusions, as though the flow of cold air is held back, or warmer air is advected inward. Moreover, an unexpected pair of elongated vorticity couplets surrounding both protrusions of cold air are seen in plots of vertical vorticity, and they appear to be channeling the cold air protrusions into narrower and more extended bands. These cyclonic/anticyclonic vorticity pairs are limited vertically to roughly the depth of the cold-air protrusions (see Figure 4c), and are collocated with elongated bands of relatively weaker upward/downward vertical motion (see Figure 4b), comparable to those seen in the simulations of, for example, Klemp and Wilhelmson (1978). However, at the front end (with respect to storm motion) of the outer vorticity maximum on each side of the storm is an updraft. With time, as the cold pools disperse and the protrusions and couplet pairs move apart, the reflectivity signature disappears.

The primary problem, then, becomes less explaining how the reflectivity signature itself forms (air rising up and over the outward-moving and rearward-advected cold outflow protrusions), but instead explaining why the vorticity couplets that advect the cold protrusions form. One possibility is that the vorticity couplets develop from tilting of vorticity by the outflow boundary— essentially creating a self-sustaining system analogous on a smaller scale to the bow-echo, bookend-vortices model illustrated by Weisman (1993). The two outward-moving initial cold pools tilt horizontal vorticity (environmental and/or solenoidally generated) into the vertical when air is lifted and descends, creating vorticity couplets which advect the cold air (and lighter precipitation particles) further rearward. Moreover, the internal vorticity pair works together in the opposite direction, advecting relatively warmer air inward, and keeping the cold air from spreading into the notch region. This hypothesis is further supported by both the TREC and ARPS analyses:

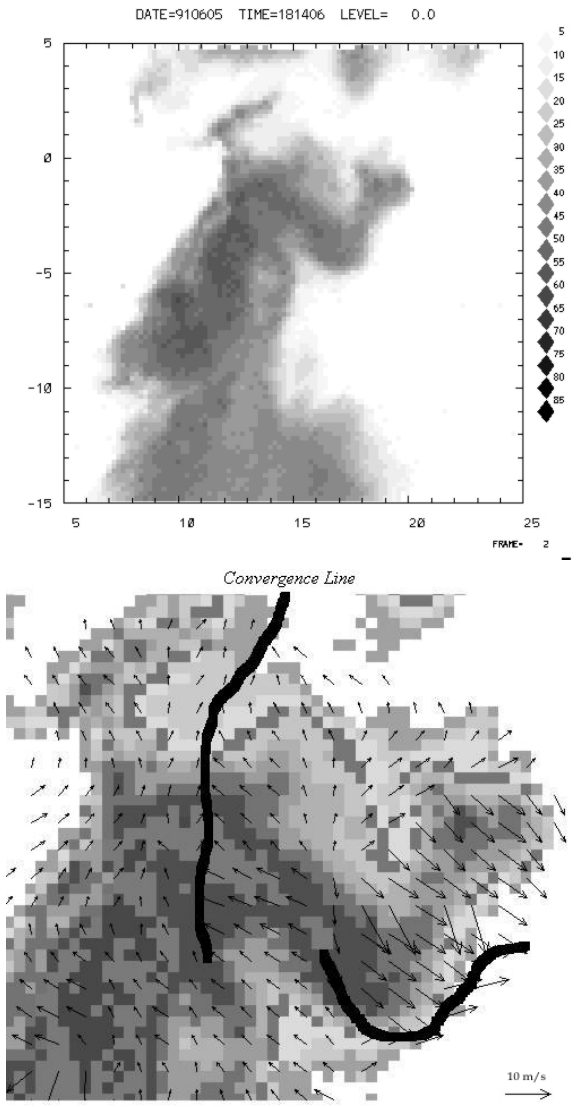

Figure 2 Same as Figure 1 but for the June 5, 2001 case. Calculations made at 5:14pm CDT

for example, in the case of May 27, the boundary is moving with greater speed at its periphery than in the center where the analyzed winds opposing its motion rearward appear to be greatest. Thus the outer edges of the boundary could progress ahead of the central parts of the boundary and coincide with the appendages in the reflectivity. Varying the shear magnitude and preserving the hodograph shape in "Owl Horn" simulation cases shows corresponding increases and decreases to the vorticity magnitudes, in further support of the tilting argument.

Both modelled storms and observed storms exhibited storm splits soon after the first appearance of the "Owl Horn" signature. However, a secondary maximum in reflectivity at the surface and a discrete second couplet of mid-level vorticity as characterize storm splitting (Bluestein, 1993) in the future left-moving storm do not appear until the "Owl Horn" is nearly fully-developed. Nevertheless, we find in plots of mid-level reflectivity a discrete secondary cell on the left side of the storm with respect to storm motion several minutes prior to the mature "Owl Horn," and we see in cross-sections the presence of a second discrete, though younger updraft.

4. SUMMARY

We have presented the characteristics of the "Owl Horn" signature and obtained a wind field by applying the TREC algorithm to our non-Doppler reflectivity data for several "Owl Horn" cases. Based on numerical simulations, it is suggested that the TREC-derived convergence line represents protrusions of cold outflow, seemingly advected by vorticity couplets which develop along the edges of the outflow. Indeed, it may be more useful to characterize the "Owl Horn" by the presence of cold protrusions in the outflow rather than by the presence of protrusions in reflectivity.

Based on Table 1, the shape and magnitude of the atmospheric shear profile play a role in the development of the "Owl Horn": supercell shear is required, though the magnitude of the shear is on the low end of the supercell shear spectrum. For completeness, we examined simulations with Adlerman and Droegemeier's (2002) cases in which low- and upper-level shear varied, preserving the shape and mean shear of the profile, and found the low-level shear seems to be of great importance, as the low-level shear cases produced "Owl Horns" while the upper-level shear cases showed no effect. The shape of the hodograph also plays a role, as the simulation cases that produced "Owl Horns" were primarily of three general types: quarter-circle, half-circle and ¾ circle. It seems also that the appearance of an "Owl Horn" signature may be aided by the presence of two initially discrete cold pools, which may be a consequence of the shape of the hodograph. Since a secondary updraft, a pair of mid-level vorticity couplets, and a secondary maximum of reflectivity are present at or prior to the time of the first sign of the "Owl Horn", we speculate that the signature in an isolated storm may signify intensification of the storm and may indicate an imminent storm-split.

Although the University of Massachusetts X-band radar was modified to include Doppler capabilities beginning in 2002, we did not encounter an "Owl Horn" signature in 2002, but did in 2003. An analysis of the new data is planned.

HODOGRAPH DESCRIPTION	RADIUS OF SHEAR WHICH PRODUCED "OWL HORN"
Half circle over 0-10 km	15, 19, 25 m/s
Half circle over 0-6 km	15, 19, 25 m/s
Quarter circle 0 to 3 km	10 m/s, tail 10 m/s,
Tail from 3 to 9km	15 m/s, tail 0, 10, 20 m/s
Straight line	None
¾ circle over 0-10 km	15, 19 m/s

Table 1: Suite of model hodographs used in numerical simulations and description of shear radii which produced "Owl Horn" signatures. (See Adlerman and Droegemeier 2002 for further details of these profiles)

5. ACKNOWLEDGMENTS

This research was funded by NSF grants ATM-9912097 at the University of Oklahoma (OU) and ATM-0000592 at U. Mass. Support was also provided by Mark Laufersweiler and staff, and the School of Meteorology at OU. Many thanks to Edwin Adlerman, Christopher Weiss, and Donald Burgess for invaluable help and advice. NCAR is supported by the National Science Foundation.

6. REFERENCES

Adlerman, E. J., and K. K. Droegemeier, 2002: The sensitivity of numerically-simulated cyclic mesocyclogenesis to variations in environmental parameters. *Preprints, 21st Conf. Severe Local Storms*, San Antonio, TX, Amer. Meteor. Soc.

Bluestein, H. B., 1993: Synoptic-Dynamic Meteorology in Midlatitudes, Vol. II. Oxford Univ. Press, 594pp.

Klemp, J. B., and R. B. Wilhelmson, 1978: Simulations of right- and left-moving storms produced through storm splitting. *J. Atmos. Sci.* **35**, 1097-1110.

Rinehart, R. E., 1979: Internal storm motions from a single non-Doppler weather radar. NCAR/TN-146+STR, 262pp.

Tuttle, J. D., and G. B. Foote, 1990: Determination of the single boundary layer airflow from a single Doppler radar. *J. Atmos. Oceanic Technol.*, **7**, 218-232.

Tuttle, J. D., and R. Gall, 1999: A single-radar technique for estimating the winds in tropical cyclones. *Bull. Amer. Meteor. Soc.*, **80**, 653-668.

Weisman, M. L., 1993: The genesis of severe, long-lived bow echoes. *J. Atmos. Sci.*, **50**, 645-670.

Xue, M., and K. K. Droegemeier and V. Wong, 2000: The Advanced Regional Prediction System (ARPS)—A multi-scale non-hydrostatic atmospheric simulation and prediction tool. Part I: Model dynamics and verification. *Meteor. Atmos. Physics*, **75**, 161-193.

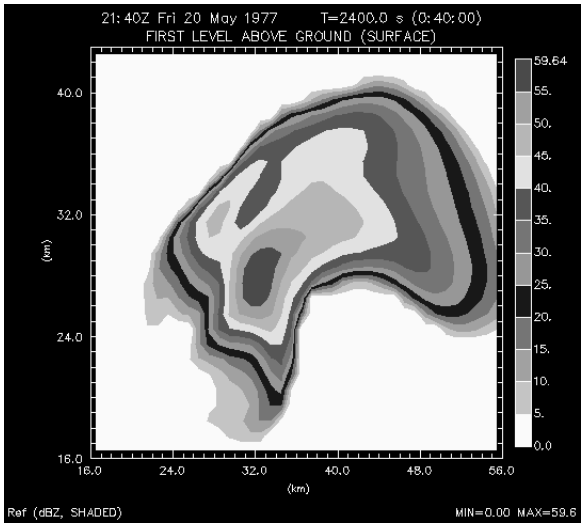

Figure 3 Plot of reflectivity at 4:40pm CDT from ARPS simulation using May 20, 1977 Del City composite sounding initialization.

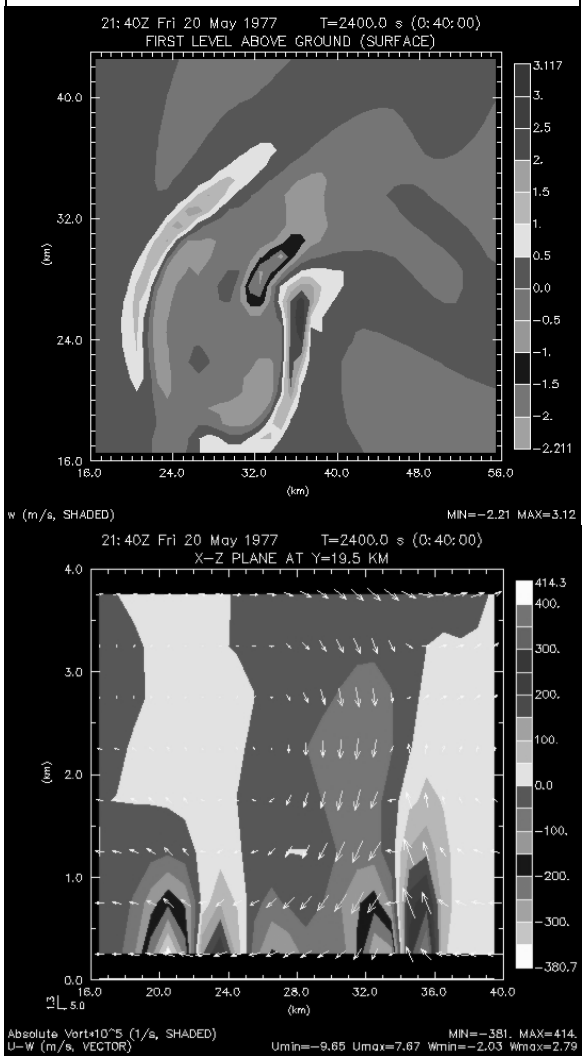

Figure 4 ARPS plots at 4:40pm CDT at the time of the most pronounced "Owl Horn" signature in reflectivity. From top: (a) perturbation potential temperature, (b) vertical motion, and (c) enlarged view of vertical cross-section of vertical vorticity and two-dimensional U-W wind.